

# Exploring the Dark Frontier: White Dwarf-Based Constraints on Light Dark Matter

Jia-Shu Niu<sup>1,2,3,\*</sup>

<sup>1</sup>*Institute of Theoretical Physics, Shanxi University, Taiyuan, 030006, China*

<sup>2</sup>*State Key Laboratory of Quantum Optics and Quantum Optics Devices, Shanxi University, Taiyuan 030006, China*

<sup>3</sup>*Collaborative Innovation Center of Extreme Optics, Shanxi University, Taiyuan 030006, China*

(Dated: June 6, 2024)

In the vast expanse of our galaxy, white dwarfs (WDs) are natural sentinels, capturing the enigmatic dark matter (DM) particles that incessantly traverse their interiors. These celestial bodies provide a unique vantage point for probing interactions between DM particles and their constituents—nuclei or electrons—should such interactions exist. The captured DM particles may accumulate, undergo mutual annihilation, or be evaporated by the WD’s own nuclei or electrons, thereby perturbing the standard cooling sequence predicted by stellar evolution theory. This letter reports pioneering constraints on DM-electron interactions derived from an in-depth analysis of four pulsating WDs. By leveraging the period variation rates of their pulsation modes, we delineate the following constraints: for a form factor  $F(q) = 1$ , in the DM mass range  $20 \text{ MeV}/c^2 \lesssim m_\chi \lesssim 80 \text{ MeV}/c^2$  with a cross-section limit of  $\sigma_{\chi,e} \lesssim 10^{-56} \text{ cm}^2$ ; for a form factor  $F(q) = (\alpha m_e)^2/q^2$ , in the DM mass range  $20 \text{ MeV}/c^2 \lesssim m_\chi \lesssim 70 \text{ MeV}/c^2$  with a limit of  $\sigma_{\chi,e} \lesssim 10^{-52} \text{ cm}^2$ . These newly established constraints surpass current direct detection experiments by over fifteen orders of magnitude, forging a path into the uncharted territories of the DM parameter space. This work not only advances our understanding of light dark matter-electron interactions but also exemplifies the potential of WDs as important astrophysical laboratories for probing the elusive nature of DM.

**Motivation.** Although dark matter (DM) is the dominant component of the matter in the Universe [1], its particle nature remains largely unknown. In recent years, candidates for DM particles have been sought through three main strategies: direct detection, indirect detection, and collider searches (for reviews, see e.g., Refs. [2–4]). Despite some suggestive signals in these searches (see e.g., Refs. [5–10] and references therein), no confirmed evidence has been obtained yet.

As the ultimate evolutionary stage of most stars in our galaxy [11], white dwarfs (WDs) possess relatively simple interior structures, consisting of an electron-degenerate core and an atmosphere envelope, and are considered to be the most promising laboratories for measuring DM-electron interactions [12].

In our galaxy, DM particles inevitably traverse WDs, losing energy upon scattering with the star’s constituents (nuclei and electrons). If these DM particles’ velocity, post deceleration, falls below the WD’s escape velocity, they become captured and gravitationally bound to the star. These captured DM particles may then accumulate, annihilate within the WD, or evaporate from it, thereby disrupting the star’s standard evolutionary trajectory as dictated by stellar evolution theory.

Fortunately, for pulsating WDs, both their interior structures and evolutionary rates can be precisely determined through the pulsation periods and their variation rates [13–16]. Consequently, DM-related processes within a WD (capture, evaporation, and annihilation) can be calculated, allowing us to predict its evolutionary rates. By comparing these predictions with observations, we can deduce the properties of DM.

**Period Variation Rates of Pulsating WDs.** The period variation rate of a pulsating WD’s pulsation mode

(denoted as  $\dot{P} \equiv dP/dt$ ), is generally described by the equation [17]:

$$\frac{\dot{P}}{P} \simeq -\frac{1}{2} \frac{\dot{T}_c}{T_c} + \frac{\dot{R}_*}{R_*}, \quad (1)$$

where  $P$  signifies the pulsation period,  $T_c$  is the core temperature of the WD, and  $R_*$  represents the WD’s radius. Utilizing the mass-radius relationship characteristic of low-mass WDs ( $R_* \propto M_*^{-\frac{1}{3}}$ ), the equation can be reformulated as:

$$\frac{\dot{P}}{P} \simeq -\frac{1}{2} \frac{\dot{T}_c}{T_c} - \frac{1}{3} \frac{\dot{M}_*}{M_*}, \quad (2)$$

with  $M_*$  being the WD’s mass.

According to Eq. (2), the impact of DM-related processes on the period variation rate  $\dot{P}$  in pulsating WDs is evident [18][19]: (a) Capture and accumulation of DM would lead to a reduction in  $\dot{P}$ , as DM particles impart kinetic energy to the star’s material ( $\dot{T}_c > 0$ ) and enhance the star’s mass ( $\dot{M}_* > 0$ ); (b) Evaporation of DM results in an increase in  $\dot{P}$ , with the star’s material transferring kinetic energy to DM particles ( $\dot{T}_c < 0$ ) and the star’s mass diminishing ( $\dot{M}_* < 0$ ); (c) Annihilation of DM decreases  $\dot{P}$ , as DM particles introduce energy into the star ( $\dot{T}_c > 0$ ) (see for e.g., [20]).

The intriguing aspect arises from contrasting the observed period variation rates with the predictions of stellar evolution for certain pulsating WDs. To date, the period variation rates for several pulsating WDs, namely G117-B15A, R548, L19-2, and PG 1351+489, have been ascertained through extensive time-series photometric observations. Yet, the observed period variation rates for the stable pulsation modes of these WDs consistently

exceed the predictions of stellar evolution theory (see Table I), suggesting a more rapid cooling progression that might be attributed to an additional cooling mechanism, such as the presence of axions [21–24].

In this study, we propose that the supplementary cooling mechanism is rooted in effective evaporation, triggered by the elastic scattering between DM particles and the WD’s constituents. While we cannot yet provide conclusive evidence for the existence of DM particles based on the observed period variation rates (see, e.g., [18]), we can cautiously rule out certain DM parameter spaces and establish constraints on the properties of DM particles.

**WDs’ Cooling by DM Evaporation.** As galactic DM particles traverse a WD, some inevitably lose energy and become captured by the star. Concurrently, these captured DM particles, having gained sufficient energy, are released back into space through evaporation.[30] The temporal evolution of the total number of DM particles within the star, denoted as  $N_\chi$ , is described by:

$$\frac{dN_\chi}{dt} = C_* - E_* \cdot N_\chi, \quad (3)$$

where  $C_*$  represents the star’s DM particle capture rate,  $E_*$  signifies the DM particle evaporation rate. The solution to Eq. (3) is given by:

$$N_\chi(t) = C_* t \cdot \left( \frac{1 - e^{-E_* t}}{E_* t} \right). \quad (4)$$

The equilibrium between capture and evaporation is examined on a timescale much shorter than that of stellar evolution. At equilibrium, the star captures and evaporates DM particles at a rate of  $C_*$  per unit time. These particles facilitate a novel pathway for energy transfer between the star and its surroundings, altering the star’s conventional cooling process.

Within a WD, the capture and evaporation rates for nuclei and electrons, represented by  $C_*$  and  $E_*$  respectively, differ due to their distinct interaction cross sections and the state of matter, with the majority of electrons existing in a Fermi degenerate state. The calculations for  $C_*$  and  $E_*$  for both nuclei and electrons are detailed in the Supplementary Material.

In a WD at equilibrium regarding DM capture and evaporation, the capture process transfers DM energy to the star, denoted as  $E^{\text{in}}$ , whereas the evaporation process transfers energy from the star to the DM and subsequently to the external environment, denoted as  $E^{\text{out}}$ . Typically, these two processes result in unequal energy exchanges, leading to a net energy change ( $E^{\text{net}} \equiv E^{\text{out}} - E^{\text{in}}$ ) for the WD at equilibrium. Observations indicate that  $E^{\text{net}} > 0$ , meaning the WDs experience a net energy loss. The specific expressions for  $E^{\text{in}}$  and  $E^{\text{out}}$  for both nuclei and electrons are provided in the Supplementary Material.

Given that electrons are significantly more efficient in mediating energy exchanges between DM particles and

the WD at equilibrium than nuclei (for further insights, refer to [18]), we disregard the capture and evaporation of DM by nuclei in our subsequent analysis.

In the equilibrium state, the number of DM particles within a WD remains constant at  $C_*/E_*$ , implying  $\dot{M}_* = 0$ . According to Eq. (2), if  $E^{\text{net}} > 0$  (which results in  $\dot{T}_c < 0$ ), an increased  $\dot{P}$  is obtained, aligning with the observed outcomes for WDs. In such a scenario, the net energy transferred can be viewed as an alternative form of luminosity, emanating from DM particles ( $L_\chi \equiv E^{\text{net}}$ ).

Drawing a parallel to the case of axions [31, 32], the relationship is expressed as:

$$\frac{\dot{P}_{\text{obs}}}{\dot{P}_{\text{the}}} = \frac{L_* + L_\chi}{L_*}, \quad (5)$$

where  $\dot{P}_{\text{the}}$  is the period variation rate as predicted by stellar evolution theory;  $\dot{P}_{\text{obs}}$  is the observed period variation rate; and  $L_*$  is the luminosity derived from asteroseismology models.

**Results and Discussions.** Utilizing the observed period variation rates from the four WDs, we employ Eq. (5) to independently delineate the excluded regions of the DM-electron interaction parameter space. As depicted in Figure 1, we present the 95% excluded lines for two scenarios of the DM form factor, namely  $F(q) = 1$  and  $F(q) = (\alpha m_e)^2/q^2$ . The bands in the figure signify the typical uncertainties associated with  $\dot{P}_{\text{the}}$ , stemming from theoretical predictions which range from  $\sim 9\% - 15\%$  [25]. In this study, we have prudently selected a 15% uncertainty to ensure a conservative approach.

The refined constraints on the DM-electron interactions are articulated as follows:

- For  $F(q) = 1$ , in the DM mass range  $20 \text{ MeV}/c^2 \lesssim m_\chi \lesssim 80 \text{ MeV}/c^2$  with a cross-section limit of  $\sigma_{\chi,e} \lesssim 10^{-56} \text{ cm}^2$ ;
- For  $F(q) = (\alpha m_e)^2/q^2$ , in the DM mass range  $20 \text{ MeV}/c^2 \lesssim m_\chi \lesssim 70 \text{ MeV}/c^2$  with a limit of  $\sigma_{\chi,e} \lesssim 10^{-52} \text{ cm}^2$ .

These constraints significantly surpass current direct detection limits, offering over fifteen orders of magnitude improvement in the  $10 - 200 \text{ MeV}/c^2$  mass range [33–41]. This advancement is attributed to the unique and advantageous configuration of WDs, which facilitates an efficient capture and evaporation of DM particles within specific mass intervals through electron interactions.

In WDs with core temperatures around  $10^7 \text{ K}$  and masses in the  $0.5 - 0.7 M_\odot$  range, characteristic of those in this study, DM particles captured by the WD’s gravity, within the  $10 - 200 \text{ MeV}/c^2$  mass range, possess kinetic energies of  $m_\chi v_{\text{esc}}^2/2$ . This energy is exactly between the thermal energy ( $\sim kT_c$ ) and the Fermi degenerate energy ( $\sim \mu_F$ ) of the electrons, rendering such WDs as ‘resonant cavities’ for DM capture and evaporation via electrons.

TABLE I. Information of the Four Pulsating White Dwarfs.

ID	G117-B15A	R548	L19-2	PG 1351+489
Marks	DAV1	DAV2	DAV3	DBV
$P_{\text{obs}}$ (s)	215.20	212.95	113.8	489.33
$P_{\text{the}}$ (s)	215.215	213.401	113.41	489.47
$\dot{P}_{\text{obs}}/P_{\text{obs}}$ (s/s)	$(5.12 \pm 0.82) \times 10^{-15}$	$(3.3 \pm 1.1) \times 10^{-15}$	$(3.0 \pm 0.6) \times 10^{-15}$	$(2.0 \pm 0.9) \times 10^{-13}$
$\dot{P}_{\text{the}}/P_{\text{the}}$ (s/s)	$1.25 \times 10^{-15}$	$1.08 \times 10^{-15}$	$1.42 \times 10^{-15}$	$0.81 \times 10^{-13}$
$M_*/M_\odot$	$0.593 \pm 0.007$	$0.609 \pm 0.012$	$0.705 \pm 0.023$	$0.664 \pm 0.013$
$\log(L_*/L_\odot)$	$-2.497 \pm 0.030$	$-2.594 \pm 0.025$	$-2.622 \pm 0.046$	$-1.244 \pm 0.030$
$\log(R_*/R_\odot)$	$-1.882 \pm 0.029$	$-1.904 \pm 0.015$	$-1.945 \pm 0.037$	$-1.912 \pm 0.015$
Distance* (pc)	57.37	32.71	20.87	175.47
Refs.	[22, 25, 26]	[22, 25–27]	[21, 23, 26, 28]	[24, 26, 29]

Note:  $P_{\text{obs}}$  is the period of a specific pulsation mode from observation,  $\dot{P}_{\text{obs}}$  is its variation rate;  $P_{\text{the}}$  is the period of a specific pulsation mode from stellar evolution theory,  $\dot{P}_{\text{the}}$  is its variation rate;  $M_*$ ,  $M_\odot$  are the mass of the WD and Sun;  $L_*$ ,  $L_\odot$  are the luminosity of the WD and Sun;  $R_*$ ,  $R_\odot$  are the radius of the WD and Sun; the distances of the WDs to the Sun are obtained based on Gaia DR3 [26].

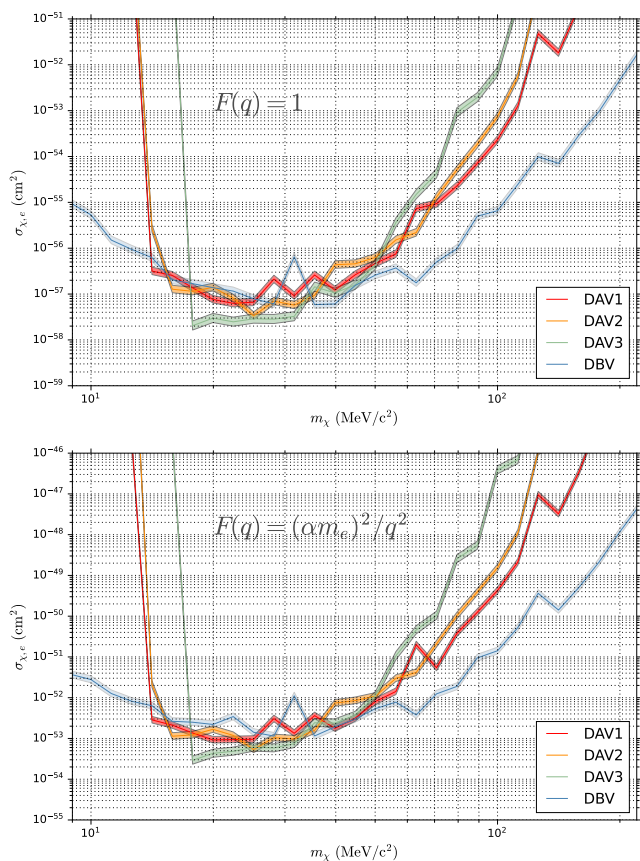


FIG. 1. 95% C.L. upper limits on DM-electron interactions as inferred from the four WDs. The scenarios for  $F(q) = 1$  (top) and  $F(q) = (\alpha m_e)^2/q^2$  (bottom) are both considered. The bands denote the uncertainties originating from  $\dot{P}_{\text{the}}$ .

Furthermore, the neutrino fog, primarily originating from solar neutrinos and typically considered a theoretical lower limit in direct DM detection experiments [42], is naturally circumvented in this scenario.

The investigative approach presented in this work may offer valuable insights for DM particle searches. It hinges

on the necessity to accurately determine the period variation rates ( $\dot{P}_{\text{obs}}$ ) of certain stable pulsation modes in pulsating WDs, thereby ascertaining their evolutionary rates. This, however, is not a straightforward task, necessitating prolonged time-series photometric observations that span decades.

Fortunately, with the growing repository of time-series photometric data from pulsating WDs, especially from space-based telescopes such as TESS, the period variation rates will be determined with increasing precision. Each dataset has the potential to provide valuable clues regarding DM particles. At the very least, it will establish an upper limit in the parameter space, contingent upon the specific properties of the WD.

We advocate for the proposal and implementation of additional innovative scenarios to perform cross-checks on the findings of this research.

J.S.N. acknowledges support from the National Natural Science Foundation of China (NSFC) (No. 12005124) and the Applied Basic Research Programs of Natural Science Foundation of Shanxi Province (No. 202103021223320).

\* jsniu@sxu.edu.cn; corresponding author

- [1] Planck Collaboration, Planck 2018 results. VI. Cosmological parameters, *Astron. Astrophys.* **641**, A6 (2020), arXiv:1807.06209 [astro-ph.CO].
- [2] J. Liu, X. Chen, and X. Ji, Current status of direct dark matter detection experiments, *Nature Physics* **13**, 212 (2016).
- [3] J. Conrad and O. Reimer, Indirect dark matter searches in gamma and cosmic rays, *Nature Physics* **13**, 224 (2017).
- [4] O. Buchmueller, C. Doglioni, and L.-T. Wang, Search for dark matter at colliders, *Nature Physics* **13**, 217 (2017).
- [5] R. Bernabei, P. Belli, F. Cappella, R. Cerulli, C. J. Dai, A. D'Angelo, H. L. He, A. Incicchitti, H. H. Kuang, J. M. Ma, F. Montecchia, F. Nozzoli, D. Prosperi, X. D. Sheng,

- and Z. P. Ye, First results from DAMA/LIBRA and the combined results with DAMA/NaI, *European Physical Journal C* **56**, 333 (2008), arXiv:0804.2741 [astro-ph].
- [6] R. Bernabei, P. Belli, F. Cappella, R. Cerulli, C. J. Dai, A. D'Angelo, H. L. He, A. Incicchitti, H. H. Kuang, X. H. Ma, F. Montecchia, F. Nozzoli, D. Prospero, X. D. Sheng, R. G. Wang, and Z. P. Ye, New results from DAMA/LIBRA, *European Physical Journal C* **67**, 39 (2010), arXiv:1002.1028 [astro-ph.GA].
- [7] A. Cuoco, M. Krämer, and M. Korsmeier, Novel dark matter constraints from antiprotons in light of ams-02, *Phys. Rev. Lett.* **118**, 191102 (2017).
- [8] M.-Y. Cui, Q. Yuan, Y.-L. S. Tsai, and Y.-Z. Fan, Possible dark matter annihilation signal in the ams-02 antiproton data, *Phys. Rev. Lett.* **118**, 191101 (2017).
- [9] J.-S. Niu, T. Li, R. Ding, B. Zhu, H.-F. Xue, and Y. Wang, Bayesian analysis of the break in DAMPE lepton spectra, *Phys. Rev. D* **97**, 083012 (2018), arXiv:1712.00372 [astro-ph.HE].
- [10] J.-S. Niu, T. Li, and F.-Z. Xu, A simple and natural interpretations of the DAMPE cosmic-ray electron/positron spectrum within two sigma deviations, *European Physical Journal C* **79**, 125 (2019), arXiv:1712.09586 [hep-ph].
- [11] G. Fontaine, P. Brassard, and P. Bergeron, The Potential of White Dwarf Cosmochronology, *Publications of the Astronomical Society of the Pacific* **113**, 409 (2001).
- [12] J. Isern, S. Torres, and A. Rebassa-Mansergas, White dwarfs as Physics laboratories: lights and shadows, *Frontiers in Astronomy and Space Sciences* **9**, 6 (2022), arXiv:2202.02052 [astro-ph.HE].
- [13] D. E. Winget and S. O. Kepler, Pulsating White Dwarf Stars and Precision Asteroseismology, *Annu. Rev. Astron. Astrophys.* **46**, 157 (2008), arXiv:0806.2573.
- [14] G. Fontaine and P. Brassard, The Pulsating White Dwarf Stars, *Publications of the Astronomical Society of the Pacific* **120**, 1043 (2008).
- [15] L. G. Althaus, A. H. Córscico, J. Isern, and E. García-Berro, Evolutionary and pulsational properties of white dwarf stars, *Astron. Astrophys. Rev.* **18**, 471 (2010), arXiv:1007.2659 [astro-ph.SR].
- [16] L. M. Calcaferro, A. H. Córscico, and L. G. Althaus, Pulsating low-mass white dwarfs in the frame of new evolutionary sequences. IV. The secular rate of period change, *Astron. Astrophys.* **600**, A73 (2017), arXiv:1701.08880 [astro-ph.SR].
- [17] D. E. Winget, C. J. Hansen, and H. M. van Horn, Do pulsating PG1159-035 stars put constraints on stellar evolution?, *Nature* **303**, 781 (1983).
- [18] J.-S. Niu and H.-F. Xue, Possible Dark Matter Signals from White Dwarfs, arXiv e-prints, arXiv:2401.04931 (2024), arXiv:2401.04931 [hep-ph].
- [19] In this analysis, we consider  $P$ ,  $T_c$ , and  $M_*$  as constants.
- [20] J.-S. Niu, T. Li, W. Zong, H.-F. Xue, and Y. Wang, Probing the dark matter-electron interactions via hydrogen-atmosphere pulsating white dwarfs, *Phys. Rev. D* **98**, 103023 (2018), arXiv:1709.08804 [astro-ph.HE].
- [21] A. H. Córscico, A. D. Romero, L. G. Althaus, E. García-Berro, J. Isern, S. O. Kepler, M. M. Miller Bertolami, D. J. Sullivan, and P. Chote, An asteroseismic constraint on the mass of the axion from the period drift of the pulsating DA white dwarf star L19-2, *J. Cosmol. Astropart. Phys.* **2016**, 036 (2016), arXiv:1605.06458 [astro-ph.SR].
- [22] A. D. Romero, A. H. Córscico, L. G. Althaus, S. O. Kepler, B. G. Castanheira, and M. M. Miller Bertolami, Toward ensemble asteroseismology of ZZ Ceti stars with fully evolutionary models, *Mon. Not. Roy. Astron. Soc.* **420**, 1462 (2012), arXiv:1109.6682 [astro-ph.SR].
- [23] D. J. Sullivan and P. Chote, The Frequency Stability of the Pulsating White Dwarf L19-2, in *19th European Workshop on White Dwarfs*, *Astronomical Society of the Pacific Conference Series*, Vol. 493, edited by P. Dufour, P. Bergeron, and G. Fontaine (2015) p. 199.
- [24] T. Battich, A. H. Córscico, L. G. Althaus, and M. M. Miller Bertolami, First axion bounds from a pulsating helium-rich white dwarf star, *J. Cosmol. Astropart. Phys.* **2016**, 062 (2016), arXiv:1605.07668 [astro-ph.SR].
- [25] S. O. Kepler, D. E. Winget, Z. P. Vanderbosch, B. G. Castanheira, J. J. Hermes, K. J. Bell, F. Mullally, A. D. Romero, M. H. Montgomery, S. DeGennaro, K. I. Winget, D. Chandler, E. J. Jeffery, J. K. Fritzen, K. A. Williams, P. Chote, and S. Zola, The Pulsating White Dwarf G117-B15A: Still the Most Stable Optical Clock Known, *Astrophys. J.* **906**, 7 (2021), arXiv:2010.16062 [astro-ph.SR].
- [26] C. A. L. Bailer-Jones, J. Rybizki, M. Fouesneau, M. Demleitner, and R. Andrae, Estimating Distances from Parallaxes. V. Geometric and Photogeometric Distances to 1.47 Billion Stars in Gaia Early Data Release 3, *Astron. J.* **161**, 147 (2021), arXiv:2012.05220 [astro-ph.SR].
- [27] A. S. Mukadam, A. Bischoff-Kim, O. Fraser, A. H. Córscico, M. H. Montgomery, S. O. Kepler, A. D. Romero, D. E. Winget, J. J. Hermes, T. S. Riecken, M. E. Kronberg, K. I. Winget, R. E. Falcon, D. W. Chandler, J. W. Kuehne, D. J. Sullivan, D. Reaves, T. von Hippel, F. Mullally, H. Shipman, S. E. Thompson, N. M. Silvestri, and R. I. Hynes, Measuring the Evolutionary Rate of Cooling of ZZ Ceti, *Astrophys. J.* **771**, 17 (2013).
- [28] G. Pajdosz, Non-evolutionary secular period increase in pulsating DA white dwarfs., *Astron. Astrophys.* **295**, L17 (1995).
- [29] A. H. Córscico, L. G. Althaus, M. M. M. Bertolami, S. O. Kepler, and E. García-Berro, Constraining the neutrino magnetic dipole moment from white dwarf pulsations, *J. Cosmol. Astropart. Phys.* **2014**, 054 (2014), arXiv:1406.6034 [astro-ph.SR].
- [30] Here, we focus on DM particles that do not annihilate.
- [31] J. Isern, M. Hernanz, and E. Garcia-Berro, Axion Cooling of White Dwarfs, *Astrophys. J. Lett.* **392**, L23 (1992).
- [32] A. H. Córscico, O. G. Benvenuto, L. G. Althaus, J. Isern, and E. García-Berro, The potential of the variable DA white dwarf G117-B15A as a tool for fundamental physics, *New Astronomy* **6**, 197 (2001), arXiv:astro-ph/0104103 [astro-ph].
- [33] Xenon Collaboration, Emission of single and few electrons in XENON1T and limits on light dark matter, *Phys. Rev. D* **106**, 022001 (2022), arXiv:2112.12116 [hep-ex].
- [34] PandaX-II Collaboration, Search for Light Dark Matter-Electron Scattering in the PandaX-II Experiment, *Phys. Rev. Lett.* **126**, 211803 (2021), arXiv:2101.07479 [hep-ex].
- [35] DAMIC-M Collaboration, First Constraints from DAMIC-M on Sub-GeV Dark-Matter Particles Interacting with Electrons, *Phys. Rev. Lett.* **130**, 171003 (2023), arXiv:2302.02372 [hep-ex].
- [36] DarkSide Collaboration, Search for Dark Matter Particle Interactions with Electron Final States with DarkSide-

- 50, *Phys. Rev. Lett.* **130**, 101002 (2023).
- [37] SENSEI Collaboration, SENSEI: First Direct-Detection Results on sub-GeV Dark Matter from SENSEI at SNOLAB, arXiv e-prints , arXiv:2312.13342 (2023), arXiv:2312.13342 [astro-ph.CO].
- [38] PandaX Collaboration, Search for Light Dark Matter with Ionization Signals in the PandaX-4T Experiment, *Phys. Rev. Lett.* **130**, 261001 (2023), arXiv:2212.10067 [hep-ex].
- [39] CDEX Collaboration, Experimental Limits on Solar Reflected Dark Matter with a New Approach on Accelerated-Dark-Matter-Electron Analysis in Semiconductors, *Phys. Rev. Lett.* **132**, 171001 (2024), arXiv:2309.14982 [hep-ex].
- [40] DAMIC-M Collaboration, Search for Daily Modulation of MeV Dark Matter Signals with DAMIC-M, *Phys. Rev. Lett.* **132**, 101006 (2024), arXiv:2307.07251 [hep-ex].
- [41] V. Zema, P. Figueroa, G. Angloher, M. R. Bharadwaj, T. Frank, M. N. Hughes, M. Kellermann, F. Pröbst, K. Schäffner, K. Shera, and M. Stahlberg, Dark Matter-Electron Scattering Search Using Cryogenic Light Detectors, arXiv e-prints , arXiv:2402.01395 (2024), arXiv:2402.01395 [hep-ph].
- [42] B. Carew, A. R. Caddell, T. N. Maity, and C. A. J. O'Hare, Neutrino fog for dark matter-electron scattering experiments, *Phys. Rev. D* **109**, 083016 (2024), arXiv:2312.04303 [hep-ph].
- [43] N. F. Bell, G. Busoni, M. E. Ramirez-Quezada, S. Robles, and M. Virgato, Improved treatment of dark matter capture in white dwarfs, *J. Cosmol. Astropart. Phys.* **2021**, 083 (2021), arXiv:2104.14367 [hep-ph].
- [44] R. Garani, Y. Genolini, and T. Hambye, New analysis of neutron star constraints on asymmetric dark matter, *J. Cosmol. Astropart. Phys.* **2019**, 035 (2019), arXiv:1812.08773 [hep-ph].
- [45] G. Busoni, A. De Simone, P. Scott, and A. C. Vincent, Evaporation and scattering of momentum- and velocity-dependent dark matter in the Sun, *J. Cosmol. Astropart. Phys.* **2017**, 037 (2017), arXiv:1703.07784 [hep-ph].
- [46] A. Gould, Weakly interacting massive particle distribution in and evaporation from the sun, *Astrophys. J.* **321**, 560 (1987).
- [47] R. Garani and S. Palomares-Ruiz, Dark matter in the Sun: scattering off electrons vs nucleons, *J. Cosmol. Astropart. Phys.* **2017**, 007 (2017), arXiv:1702.02768 [hep-ph].

## Supplementary Material

### Exploring the Dark Frontier: White Dwarf-Based Constraints on Light Dark Matter

Jia-Shu Niu

In this supplementary section, we provide an exhaustive account of the capture and evaporation rates for DM particles, denoted as  $C_*$  and  $E_*$ , respectively, as well as the energy transferred during these processes,  $E^{\text{in}}$  and  $E^{\text{out}}$ .

#### CAPTURE AND EVAPORATION RATES OF DM PARTICLES

Generally, there exists an upper bound on the capture rate of a WD for DM particles, defined under the scenario where every DM particle passing through the star is captured. This condition of saturated capture is referred to as the geometric limit, expressed by the equation [43]:

$$C_{\text{geo}} = \frac{\pi R_*^2}{3v_*} \frac{\rho_\chi}{m_\chi} \left[ (3v_{\text{esc}}^2(R_*) + 3v_*^2 + v_d^2) \cdot \text{Erf} \left( \sqrt{\frac{3}{2}} \frac{v_*}{v_d} \right) + \sqrt{\frac{6}{\pi}} v_* v_d \cdot \exp \left( -\frac{3v_*^2}{2v_d^2} \right) \right]. \quad (6)$$

Here, the local DM density around the Sun is denoted by  $\rho_\chi = 0.3 \text{ GeV/cm}^3$ ;  $m_\chi$  represents the mass of the DM particle;  $R_*$  is the star's radius;  $v_{\text{esc}}(r)$  is the escape velocity of a DM particle at a distance  $r$  from the star's center;  $v_* = 220 \text{ km/s}$  is the Sun's relative velocity with respect to the DM frame where the average DM speed is null; and  $v_d = 270 \text{ km/s}$  is the dispersion velocity of DM particles in the vicinity of the Sun. Given the relatively small distances from the Sun to the four WDs compared to the galactic center ( $\sim 8.5 \text{ kpc}$ ), the values of  $\rho_\chi$ ,  $v_*$ , and  $v_d$  are considered constant throughout this study.

In the non-saturation capture condition, the capture rate of DM particles is formulated as follows [43, 44]:

$$C_{\text{ngeo}} = \int_0^{R_*} \frac{\rho_\chi}{m_\chi} 4\pi r^2 dr \int_0^\infty \frac{f_{v_*}(u_\chi)}{u_\chi} w(r) du_\chi \int_0^{v_{\text{esc}}} R^-(w \rightarrow v) dv, \quad (7)$$

where  $u_\chi$  represents the velocity of DM particles at a significant distance from the star;  $w(r) = \sqrt{u_\chi^2 + v_{\text{esc}}^2(r)}$  signifies the velocity of a DM particle at an arbitrary distance from the star's center;  $R^-(w \rightarrow v)$  denotes the differential scattering rate for capture, considering a DM particle with initial velocity  $w$  scattering to a lower velocity  $v$  ( $w > v$ ), a process that is contingent upon the star's material equation of state and varies between nuclei and electrons;  $f_{v_*}(u_\chi)$  is the DM velocity distribution, typically characterized by a Maxwell-Boltzmann distribution [45]:

$$f_{v_*}(u_\chi) = \frac{u_\chi}{v_*} \sqrt{\frac{3}{2\pi(v_d^2 + 3kT_*/m_T)}} \left( \exp \left[ -\frac{3(u_\chi - v_*)^2}{2(v_d^2 + 3kT_*/m_T)} \right] - \exp \left[ -\frac{3(u_\chi + v_*)^2}{2(v_d^2 + 3kT_*/m_T)} \right] \right), \quad (8)$$

In this context,  $k$  symbolizes the Boltzmann constant;  $T_*$  refers to the temperature of the star, which is generally radius-dependent;  $m_T$  is the mass of the target particles, which could be either nuclei or electrons.

The capture rate is generally defined as the minimum of the geometric and non-geometric capture rates:

$$C_* = \min\{C_{\text{geo}}, C_{\text{ngeo}}\}. \quad (9)$$

The evaporation rate is articulated with precision in the following equation [45–47]:

$$E_* = \int_0^{R_*} n_\chi(r) 4\pi r^2 dr \int_0^{v_{\text{esc}}} f_\chi(w, r) 4\pi w^2 dw \int_{v_{\text{esc}}}^\infty R^+(w \rightarrow v) dv, \quad (10)$$

where  $R^+(w \rightarrow v)$  represents the differential scattering rate for evaporation, contingent upon the target particles within the star;  $n_\chi(r)$  denotes the normalized radial distribution of DM [44, 46, 47]:

$$n_\chi(r) = \frac{4}{r_\chi^3 \sqrt{\pi}} \exp \left( -\frac{r^2}{r_\chi^2} \right), \text{ with } r_\chi = \sqrt{\frac{3kT_*}{2\pi G\rho_* m_\chi}}, \quad (11)$$

$G$  being the gravitational constant, and  $\rho_*$  symbolizing the star's density;  $f_\chi(w, r)$  is the velocity distribution of the thermalized DM particles, conforming to a Maxwell-Boltzmann distribution truncated at the escape velocity  $v_{\text{esc}}(r)$  as delineated by [44, 46, 47]:

$$f_\chi(w, r) = \frac{1}{\pi^{3/2}} \left( \frac{m_\chi}{2kT_*} \right)^{3/2} \frac{\exp\left(-\frac{m_\chi w^2}{2kT_*}\right) \Theta(v_{\text{esc}}(r) - w)}{\text{Erf}\left(\sqrt{\frac{m_\chi v_{\text{esc}}^2(r)}{2kT_*}}\right) - \frac{2}{\sqrt{\pi}} \sqrt{\frac{m_\chi v_{\text{esc}}^2(r)}{2kT_*}} \exp\left(-\frac{m_\chi v_{\text{esc}}^2(r)}{2kT_*}\right)}. \quad (12)$$

In the domain of nuclear interactions, the differential scattering rates for capture and evaporation are defined as follows [45]:

$$R^-(w \rightarrow v) = \frac{32\mu_+^4}{\sqrt{\pi}} \kappa^3 n_n(r) \frac{d\sigma_N}{d\cos\theta} \frac{v}{w} \int_0^\infty dv_s \int_0^\infty v_t e^{-\kappa^2 v_t^2} H^-(v_s, v_t, w, v) dv_t, \quad (13)$$

and

$$R^+(w \rightarrow v) = \frac{32\mu_+^4}{\sqrt{\pi}} \kappa^3 n_n(r) \frac{d\sigma_N}{d\cos\theta} \frac{v}{w} \int_0^\infty dv_s \int_0^\infty v_t e^{-\kappa^2 v_t^2} H^+(v_s, v_t, w, v) dv_t. \quad (14)$$

The associated parameters are detailed as:

$$\begin{aligned} \mu_\pm &= \frac{\mu \pm 1}{2}, \mu = \frac{m_\chi}{m_n}, \kappa^2 = \frac{m_n}{2kT_*}, \\ v_T^2 &= 2\mu\mu_+v_t^2 + 2\mu v_s^2 - \mu w^2, \\ H^-(v_s, v_t, w, v) &= \Theta(v_t + v_s - w)\Theta(v - |v_t - v_s|), \\ H^+(v_s, v_t, w, v) &= \Theta(v_t + v_s - v)\Theta(w - |v_t - v_s|), \end{aligned} \quad (15)$$

In these expressions,  $n_n(r)$  signifies the number density of the nucleus;  $v_s$  denotes the velocity in the star's frame of the center of mass (CM) of the scattering event, while  $v_t$  is the velocity of the DM in the CM frame;  $m_n$  is the mass of the nucleus.

For electrons, the differential scattering rates for capture and evaporation can be expressed as [44]

$$R^-(w \rightarrow v) = 8\mu_+^4 \sigma_{\chi,e} F(q) n_e(r) \frac{v}{w} \int_0^\infty dv_s \int_0^\infty v_t f_p(E_p, r) (1 - f_{p'}(E_{p'}, r)) H^-(v_s, v_t, w, v) dv_t, \quad (16)$$

and

$$R^+(w \rightarrow v) = 8\mu_+^4 \sigma_{\chi,e} F(q) n_e(r) \frac{v}{w} \int_0^\infty dv_s \int_0^\infty v_t f_p(E_p, r) (1 - f_{p'}(E_{p'}, r)) H^+(v_s, v_t, w, v) dv_t, \quad (17)$$

where the parameters are defined as:

$$\begin{aligned} \mu_\pm &= \frac{\mu \pm 1}{2}, \mu = \frac{m_\chi}{m_e} \\ f_p(E_p, r) &= \left( \exp\left(\frac{E_p - \mu_F(r)}{T_*}\right) + 1 \right)^{-1}, \\ 1 - f_{p'}(E_{p'}, r) &= 1 - \left( \exp\left(\frac{E_{p'} - \mu_F(r)}{T_*}\right) + 1 \right)^{-1}, \\ E_p &= \frac{1}{2} m_e (2\mu\mu_+v_t^2 + 2\mu v_s^2 - \mu w^2), \\ E_{p'} &= \frac{1}{2} m_e (2\mu\mu_+v_t^2 + 2\mu v_s^2 - \mu w^2), \end{aligned} \quad (18)$$

In these expressions,  $n_e(r)$  signifies the number density of electrons;  $m_e$  is the electron's mass;  $f_p(E_p, r)$  and  $1 - f_{p'}(E_{p'}, r)$  represent the Fermi-Dirac distribution for the electron in its initial and final states, respectively;  $\mu_F(r)$  is the chemical potential of the electron at position  $r$ ;  $H^\pm(v_s, v_t, w, v)$  is consistent with the expression given in Eq. (15);  $F(q)$  is the DM form factor dependent on momentum.

For the scope of this research, two scenarios are considered for the DM form factor:  $F(q) = 1$  and  $F(q) = (\alpha m_e)^2/q^2$ , where  $\alpha$  is the fine-structure constant and  $q$  denotes the transferred momentum.

Additionally, several simplifying assumptions have been applied in our analysis: (i) We assume a uniform matter distribution within a WD, expressed as  $\rho_*(r) = \rho_* = M_*/V_*$ , where  $\rho_*$ ,  $M_*$  and  $V_*$  represent the density, mass, and volume of a WD, respectively. (ii) Given that all four WDs considered in this study are carbon-oxygen core WDs, we adopt a uniform chemical composition across the scattering volume  $V_*$ , utilizing an average atomic weight of 14 for the nucleus [27]. (iii) We also assume a uniform temperature profile  $T_*$  within a WD, which is independent of the radial distance  $r$ , due to the exceptionally high thermal conductivity of the electron-degenerate core. (iv) Considering that WDs are electrically neutral, we calculate the total number of electrons  $N_e$  and the number density of electrons  $n_e$  in a WD using the expressions  $M_*/2m_p$  and  $\rho_*/2m_p$ , respectively, where  $m_p$  is the mass of a proton.

### ENERGY TRANSFERRED BY DM CAPTURE AND EVAPORATION

The kinetic energy transferred to the star's nuclei or electrons during the capture process is articulated by the following expression, applicable when  $C_{\text{geo}} < C_{\text{ngeo}}$ :

$$E^{\text{in}} = \frac{C_{\text{geo}}}{C_{\text{ngeo}}} \int_0^{R_*} \frac{\rho_\chi}{m_\chi} 4\pi r^2 dr \int_0^\infty \frac{f_{v_*}(u_\chi)}{u_\chi} w(r) du_\chi \int_0^{v_{\text{esc}}} \frac{1}{2} m_\chi (w^2 - v^2) \cdot R^-(w \rightarrow v) dv. \quad (19)$$

For scenarios when  $C_{\text{geo}} \geq C_{\text{ngeo}}$ , the energy transferred during capture is given by:

$$E^{\text{in}} = \int_0^{R_*} \frac{\rho_\chi}{m_\chi} 4\pi r^2 dr \int_0^\infty \frac{f_{v_*}(u_\chi)}{u_\chi} w(r) du_\chi \int_0^{v_{\text{esc}}} \frac{1}{2} m_\chi (w^2 - v^2) \cdot R^-(w \rightarrow v) dv. \quad (20)$$

The kinetic energy transferred from the WD's constituents to the DM particles during the evaporation process is described by:

$$E^{\text{out}} = C_* \int_0^{R_*} n_\chi(r) 4\pi r^2 dr \int_0^{v_{\text{esc}}} f_\chi(w, r) 4\pi w^2 dw \int_{v_{\text{esc}}}^\infty \frac{1}{2} m_\chi (v^2 - w^2) \cdot R^+(w \rightarrow v) dv. \quad (21)$$

These expressions are derived from the foundational equations (13), (14), (16), and (17).